Chemical-Mechanical Polishing and Material Characteristics of Plasma-Enhanced Chemically Vapor Deposited Fluorinated Oxide Thin Films

Wei-Tsu Tseng,[a] Yuan-Tsu Hsieh,[b,c] Chi-Fa Lin,[b,c] Ming-Shih Tsai,[a] and Ming-Shiann Feng[b]

[a]National Nano Device Laboratories and [b]Institute of Materials Science and Engineering, National Chiao-Tung University, Hsinchu 300, Taiwan

ABSTRACT

The chemical-mechanical polishing (CMP) process has been proven to be the most promising method for accomplishing global planarization. In this paper, results of chemical-mechanical polishing of fluorinated silicon dioxide (SiOF) thin films are presented. Nanohardness, elastic modulus, and bonding structure of fluorinated silicon dioxides are characterized in order to evaluate their correlations with CMP performance. The results show that under fixed chemistry and mechanical parameters, the CMP removal rate increases significantly with increasing fluorine content in the oxides due to the lower hardness and elastic modulus in the films. Higher CMP removal rate is observed for fluorinated oxides polished with slurry of pH 10 relative to pH 9. Compared with undoped oxides, SiOF films are more sentisitive to chemical and moisture attacks as reflected by the post-CMP increase in refractive index.

Introduction

Advanced semiconductor device interconnects are the pivotal components governing the final device yield and reliability. The trend toward shrinking design rules and increasing interconnect packing density have driven the development of multilevel interconnect systems. As interconnect lines shrink and move closer together, the resistance of conductor lines and plugs and the capacitance of SiO_2-based intermetal dielectrics limit further increase in clock speed.[1] The incorporation of low permittivity (low-ϵ) dielectrics and lower resistance, electromigration-immune conductors into the interconnect scheme has become imperative to further reduce the RC delay in the deep submicron regime.[2] Recently, many low-ϵ materials based on totally different chemistries such as polymides have been put forth.[3,4] Meanwhile, new film formation technologies are being invented to improve the quality of the traditional SiO_2-based intermetal dielectrics (IMD) while reducing their dielectric constants by fluorine doping. These include plasma-enhanced chemical vapor deposition (PECVD),[5,6] liquid-phase deposition (LPD),[7] tetraethoxysilane-ozone (TEOS-O_3), atmospheric-pressure chemical vapor deposition (AP-CVD),[8] room temperature catalytic CVD (RT-CVD),[9-11] and spin-on glasses (SOG).

Despite the different approaches to low-ϵ dielectrics, potential IMDs for future ultralarge scale integrated (ULSI) applications should all meet a number of other material requirements such as low stress, good thermal stability, and minimal moisture permeation. Additionally, they must be compatible with advanced ULSI planarization technologies like chemical-mechanical polishing (CMP) from a process integration point of view. The CMP characteristics of the fluorine-doping oxide films have been reported previously.[12,13] However, knowledge of the mechanical characteristics of SiOF films is still obscure and insufficient for evaluating the role of mechanical abrasion during CMP of fluorinated oxides. Besides, lots of previous studies have found that SiOF films are easily attacked by moisture. Since, during CMP operation, the samples are immersed in an aggressive aqueous slurry, the stability of SiOF films during CMP is an issue. Hence the feasibility of SiOF-CMP becomes a subject for further investigation.

In this article, results of chemical-mechanical polishing of SiOF thin films are presented. Nanohardness, elastic modulus, and bonding structure of fluorinated silicon dioxides are characterized in order to evaluate their correlations with CMP performance. An alkaline-based slurry with adjusted pH was used for polishing in an attempt to delineate the chemical erosion from mechanical abrasion effects during CMP of SiOF films. Finally, changes in refractive index, surface morphology, and bonding density after CMP were recorded to evaluate the chemical stability and CMP viability of low-ϵ SiOF dielectric thin films.

[c] Present address: Winbond Electronics Corporation, Science-Based Industrial Park, Hsinchu 300, Taiwan.

Experimental

Preparation of SiOF films.—All test samples in the present study were deposited on p-type (100), 150 mm silicon wafers in a Novellus dual frequency PECVD reactor with TEOS/O_2/C_2F_6 chemistry. The high frequency (13.56 MHz) was used to generate the plasma and the low frequency (0.375 MHz) was used to enhance the ion bombardment of the deposited films. The SiOF films with different fluorine content were obtained by adjusting the C_2F_6 flow rate from 0.8 to 4.8 liter per minute while fixing the TEOS and O_2 flow rates at 0.0023 and 10 liter per minutes, respectively. The chamber pressure was 2.6 Torr and the substrate temperature was 400°C. All specimens were deposited to a thickness of about 1 μm.

Polisher setup.—A Westech Model 372M CMP processor, consisting of an IC 1000/Suba IV (made of polyurethane impregnated polyester) pad affixed to a circular polishing table, and a carrier to hold wafers against the pad was used for polishing. During the polishing experiment, the wafer was mounted on a template assembly for a single 6 in. diam wafer. The Teflon retaining ring is recessed from the wafer surface by 7 mils. Pressure at the wafer-slurry-pad interface is controlled via an overhead mechanism which allows pressure to be applied to the wafer holder. Both the carrier and table were rotated independently. The thickness and refractive index of the dielectric films were measured by a Nanospec 210XP thickness measurement system. The thickness was averaged over nine measurement points to determine the polish rate.

Pad conditioning.—Pad conditioning techniques were used to refurbish the pad surface to maintain the removal rate without sacrificing uniformity. In our experiments, pad conditioning with Rotating Pad Conditioner II was performed between each wafer to clean the slurry residue and to lift the pad fibers for further processing. Without this procedure, the polish rate decreased substantially after only several wafers. Our polishing experiments were carried out under well-controlled conditions, *e.g.*, pad conditioning was performed before and between each wafer, and polishing was terminated before pad glazing could cause a significant decrease in removal rate.

Downloaded on 2014-04-28 to IP 140.113.38.11 address. Redistribution subject to ECS terms of use (see ecsdl.org/site/terms_use) unless CC License in place (see abstract).

Slurry preparation.—Slurry composition, flow rate, and the direction of slurry impingement onto the polish pad play important roles in the interlevel dialectric (ILD) CMP removal rate. The pH of the slurry is especially important in controlling the etching characteristics and chemical erosion during CMP of the wafers. The slurry pH also affects the dispersion of silica particles significantly. The particles attain a surface charge, the sign and magnitude of which depend on the pH of the solution. As pH increases, the zeta potential (the actual potential a few angstroms away from the surface) of the particles decreases, becoming negative for pH above the isoelectric point.[14] Up to pH 7.5, the viscosity of the silica slurry in an aqueous medium is very high. Beyond pH 7.5, the silica particles attain sufficient surface charge to generate electrostatic repulsion and effectively disperse the slurry. Finally, at pH greater than 10.7, the particles dissolve and form silicate.[15] Within the limits, a higher concentration of hydroxyl ions in the slurry significantly increase the ILD etch rate.

In our experiments, the CMP removal rates with variations in slurry pH (9 and 10) and down force pressure (4 to 17 psi) were monitored in order to assess the roles of chemical erosion and mechanical abrasion during CMP of SiOF films. The polish slurry (SC-1 slurry available from Rippey Corporation) was a suspension of fumed silica dispersed in aqueous potassium hydroxide. The SC-1 slurry pH is adjusted by HNO_3 solution. The pH decreased linearly with the increasing volume of HNO_3 added. The slurry remains stable in the pH range between 10.3 to 8.4 while suspensions occur when the pH value gets below 8.4. Therefore the pH values are set at 9 and 10 in order to attain stable and consistent removal rate data for studies of the chemical erosion effects during CMP.

Nanoidentation measurement.—A NanoTest 500 microprobe system with a Berkovich-type indenter is used for nanohardness determination. The elastic modulus is calculated from the elastic recovery parameter[16] R defined as

$$R = (2E)^{-1}H(1 - \nu^2)(K\pi)^{1/2}$$

where E is the elastic modulus, H is the nanohardness, υ is the Poisson's ratio, and K is the indenter shape factor which is 23.897 for Berkovich indenters. In this work, the loading rate was set at 1.2 mN/s to a maximum depth of 600 nm and the ambient temperature was held at 22.7°C. For this study, it was assumed that the substrate did not significantly affect the modulus value obtained by indenting into the first 400 nm of the 1 μm thick films. For each sample, five separate indents, spaced 20 μm apart from each other, were made on the surface under investigation.

Material characterization.—Chemical, physical, and electric properties of the film, such as refractive index, residual stress, wet etching rate, chemical bonding structure, fluorine content, dielectric constant, nanohardness, and elastic modulus were investigated using approximately 1.0 μm thick films on Si substrates. The residual stress was calculated from the following formulae

$$\sigma = \frac{E}{(1 - \nu)} \frac{h_s^2}{6Rh_f}$$

where σ, E, υ, h_s, h_f, and R are film stress, Young's modulus of Si, Poisson's ratio of Si, Si substrate thickness, film thickness, and radius of curvature, respectively. The radius of the curvature was measured by a FLX 2320 stress measurement system. The wet etching rate of the SiOF film was determined using a 10:1 buffered buffered oxide etch (BOE) aqueous solution. A Fourier transform infrared (FTIR) measurement system, Model QS-300 (Bio-Rad), was employed for investigating the chemical bonding structure and Si-F bond concentration. Bare silicon wafers were used as the references for FTIR measurements before TEOS-oxide or fluorinated oxide deposition. The dielectric constant was calculated from the maximum capacitance evaluated from a 1 MHz capacitance-voltage measurement.

Results and Discussion

Figure 1 showed the FTIR spectra of SiOF films over a wave number range between (Fig. 1a) 400 ~ 1400 cm^{-1} and (Fig. 1b) 2000 ~ 3800 cm^{-1}. The labels A to E represent the Si–F concentration at 2.4, 4.2, 5.8, 7.5, and 8.9 atom percent (a/o), respectively. As depicted, the absorption peaks at around 1070, 815, and 445 cm^{-1} corresponding to the Si–O bond-strengthening mode, Si–O bond-bending mode, and Si–O bond-rocking mode are observed, respectively. The absorption peak at around 940 cm^{-1}, which corresponds to the Si–F stretching mode, is also present. As depicted in Fig. 1a, the peak height of Si–F bond increases with the increase in the C_2F_6 flow rate. These Si–F bonds were formed during the surface anisotropic etching by C_2F_6 plasma. Most of them were evaporated while some remained on the surface and were incorporated in the oxide structure.[5] In addition, the peak position of Si–O bond (stretching mode) moves slightly toward higher wave numbers and width of the Si–O band decreases with the concurrent increase in peak height of the Si–F bonds. As shown in Fig. 1b, the Si–OH bonds at wave numbers around 3650 cm^{-1} are also present. The absorption peak height of the Si–OH bonds in the as-deposited SiOF films decreases with the increasing fluorine concentration.[16] However, after being exposed to the clean room ambient for 72 h, the Si–OH peak height of these SiOF films with higher fluorine content is found to increase due to a higher amount of moisture intake relative to the undoped PE-TEOS oxides. Finally, absorption peaks corresponding to organic compounds are not found in the SiOF films.

The presence of the highly (in fact, the most) electronegative fluorine ions in the SiO_2 network induces remarkable impacts on the electrical, mechanical, and chemical properties of the oxide. As depicted in Fig. 2, as fluorine is being doped into the SiO_2 network, electrons of the O–Si(1) bonds in the O–Si(1)–F structure move toward the fluorine side under the influence of the strong electronegativity. This electron shift leads to the enhancement in O–Si(1) bond strength with the formation of d-p π back bonding and the weakening in strength in the neighboring Si–O bonds (for example, the Si(2)–O bond as shown in Fig. 2). As a consequence, the entire oxide network becomes less polarizable, which gives rise to the lowering of dielectric constant and refractive index. The weakening of the bridging Si(2)–O bonds in Fig. 2 also implies the deterioration of the Si–O tetrahedra network inside the oxides and hence the reduction in the hardness and mechanical strength of the fluorinated oxides as well. In addition, the high hydrophilicity of fluorine enhances the moisture absorption of the oxides. The formation of HF upon moisture intake poses deep concerns over metal corrosion and degradation of the oxide itself.

Table I summarizes the material properties of SiOF films with TEOS + O_2 + C_2F_6 chemistries deposited in a dual-frequency plasma process. The dielectric constant and refractive index both decrease as more fluorine becomes present in the oxides. The addition of fluorine also switches the intrinsic stress from medium compressive (176 MPa) in undoped TEOS oxides to low tensile (35 MPa) in heavily doped (~8.9 a/o) SiOF oxides. This shift in stress may have potential technical merits since it provides, by adequate fluorine-doping, a simple way to fine tune (or to alleviate) the stress level in the IMDs with a concurrent decrease in the dielectric constant. Hardness of the oxides declines with increasing fluorine content as explained previously. This reduction in hardness is also coupled with the decrease in elastic modulus. Additionally, wet etch rates of these oxides tested by 10:1 BOE solution scale up with the added fluorine content. This can be rationalized by a "self-assisted etching" mechanism described later due to the formation of HF in the fluorinated oxides when they are immersed in the BOE solution.[9]

The alterations in material characteristics by the addition of fluorine into the PECVD oxides would certainly affect the CMP performance of this new low-ϵ dielectric.

Downloaded on 2014-04-28 to IP 140.113.38.11 address. Redistribution subject to ECS terms of use (see ecsdl.org/site/terms_use) unless CC License in place (see abstract).

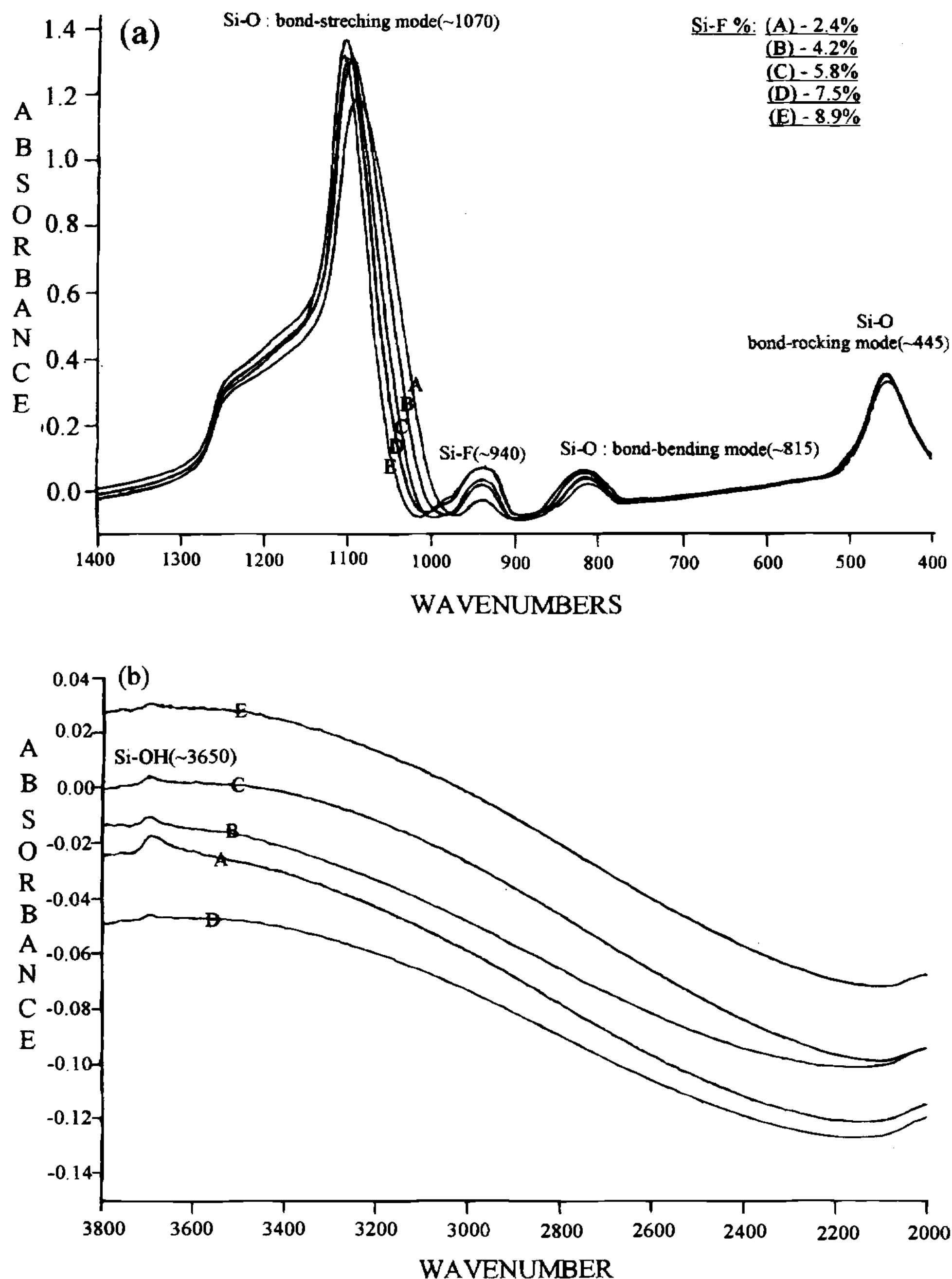

Fig. 1. FTIR spectra of pre-CMP SiOF films at two wave number ranges. (a) 400 ~ 1400 cm^{-1} and (b) 2000 ~ 3800 cm^{-1}.

Since the SiOF films become mechanically softer and less stiff as more Si–F bonds are incorporated into the O–Si–O network, the rigid particles in CMP slurry (usually silica for oxide CMP) would abrade the oxide surface more efficiently leading to a higher mechanical abrasion rate. Similarly, the high chemical reactivity of fluorine with moisture and alkaline-based solutions (common slurry chemistry) implies that the chemical erosion rate would be enhanced as well. From both mechanical and chemical aspects, an elevated CMP removal rate of SiOF films is expected compared with that of undoped oxides.[17]

The CMP removal rates under a fixed pressure of 7 psi (48,260 Pa) for SiOF films of different fluorine concentration are shown in Fig. 3. Removal rates with Cabot's SC-1 slurry of pH 9 and 10 are both recorded. The presence of fluorine in the oxides not only enhances the removal rate significantly but also sensitizes the oxides to slurry pH value. Higher removal rates are observed with the slurry of pH 10 as more fluorine is added to the oxides. This may result from the accelerated chemical reactions between the higher pH alkaline based slurry and the SiOF films with higher fluorine content (increased acidity).

The variations in removal rate with the applied down pressure for undoped and fluorine-doped TEOS oxides are depicted in Fig. 4a and b for slurry with pH 10 and pH 9, respectively. In both cases, removal rates are found to be more sensitive to the variations in down pressure in SiOF films than in undoped oxides. These results can be justified on the basis of enhanced chemical reactivity and reduced hardness and modulus in SiOF films. According to the Preston equation[18]

$$\text{Removal rate} = K_P \times PV$$

(where K_p is the Preston coefficient, P is the applied down pressure, and V is rotation speed), the first derivative of removal rate to applied down pressure at constant platen speed (20 rpm in the present study) signifies the weighing factor which accounts for the degree of chemical erosion and material effects to the overall material removal, besides the contribution of pressure and speed. Therefore, in the present case, the greater slope of the removal rate *vs.* pressure line for fluorine-doped oxides relative to undoped oxides provides further support for the hypothesis

Downloaded on 2014-04-28 to IP 140.113.38.11 address. Redistribution subject to ECS terms of use (see ecsdl.org/site/terms_use) unless CC License in place (see abstract).

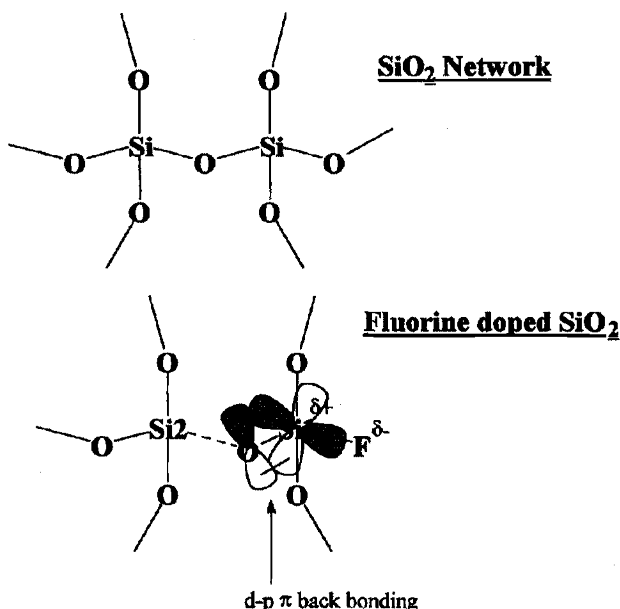

Fig. 2. A schematic diagram showing the formation of Si–F bonds in the oxide network. The enforcement of the bonding between the oxygen atom with the first silicon (denoted as Si1) atom in the presence of Si–F bonds weakens the neighboring Si–O (denoted as Si2–O) bond.

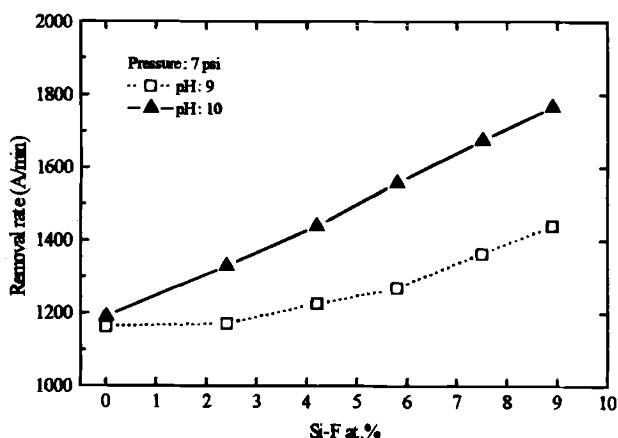

Fig. 3. The CMP removal rates of SiOF films with different fluorine concentrations under a constant pressure of 7 psi.

that CMP removal rate enhancement of the fluorinated oxides is due to their higher chemical reactivity and reduced hardness and modulus.

As mentioned earlier, moisture absorption can be a serious problem for the stability of SiOF films. Since, during the CMP process, wafers are in intimate contact with an aggressive aqueous slurry, post-CMP property changes resulting from moisture absorption may be one of the critical issues to determine the feasibility of CMP for SiOF films. Figure 5a shows the post-CMP changes in refractive

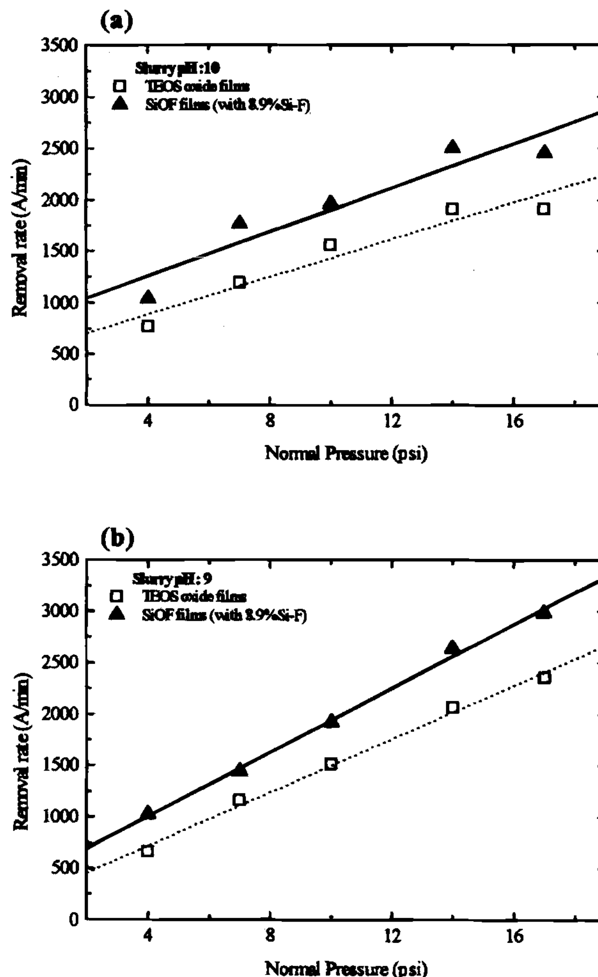

Fig. 4. The variations in CMP removal rate with applied pressure for undoped and F-doped TEOS oxides. (a) Polishes with slurry of pH 10, (b) polishes with slurry of pH 9.

index (R.I.) as a function of the Si–F concentration in oxides. A remarkable increase in R.I. can be seen after CMP for SiOF films with Si–F concentration greater than ~5.8 a/o. This change in R.I. may arise from accelerated chemical reactions and exacerbated moisture attack during CMP, but not from mechanical effects such as changes in surface roughness/scratching due to increasing pressure. The R.I. change *vs.* pressure plot in Fig. 5b provides indirect evidence for this point. As shown, the changes in R.I for SiOF films of 8.9 a/o Si–F after CMP are virtually unaffected by the variation in down pressure. The mechanical influence in the post-CMP R.I. increase is thus minimal, if any. The FTIR spectra in Fig. 6a shows a slight shift in the peak positions of both Si–O stretching (wave number from 1100 to 1102 cm^{-1}) and Si–F stretching (wave number from 928 to 927 cm^{-1}) modes after CMP for SiOF with 8.9 a/o Si–F. These shifts in frequency, though marginal, may be associated with chemical modifications in post-CMP SiOF with Si–F bond concentration greater than 5.8 a/o.

Table I. Pre-CMP material characteristics of fluorinated oxide thin films.

C_2F_6 flow rate	TEOS (undoped)	0.8 liter/min	2.0 liter/min	3.0 liter/min	4.0 liter/min	4.8 liter/min
Si-F a/o	0.0	2.4	4.2	5.8	7.5	8.9
Refractive index	1.4441	1.4310	1.4280	1.4137	1.4066	1.3910
Dielectric Constant	4.20	3.92	3.67	3.45	3.28	3.19
Stress (MPa)	−176	−135	−68	−36	15	35
Nanohardness (GPa)	20.41	17.65	—	13.27	11.86	11.03
Elastic Modulus (GPa)	167	154	—	131	100	97
Etch rate (nm/min)	110	310	492	915	1180	1350

Downloaded on 2014-04-28 to IP 140.113.38.11 address. Redistribution subject to ECS terms of use (see ecsdl.org/site/terms_use) unless CC License in place (see abstract).

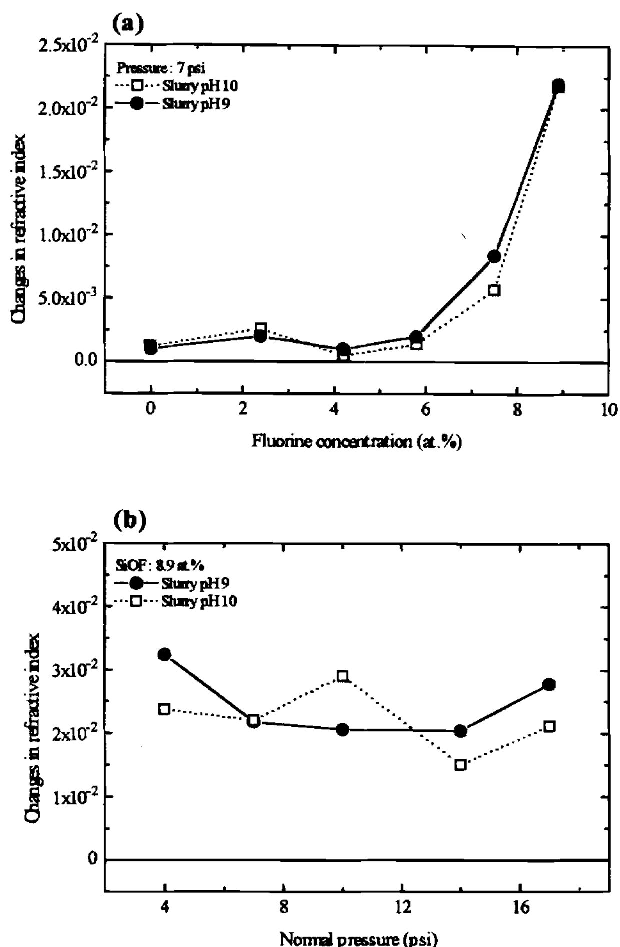

Fig. 5. Refractive index (R.I.) increases after CMP. (a) R.I. changes vs. fluorine concentration under 7 psi pressure. (b) R.I. changes vs. applied pressure for SiOF with 8.9 a/o Si–F.

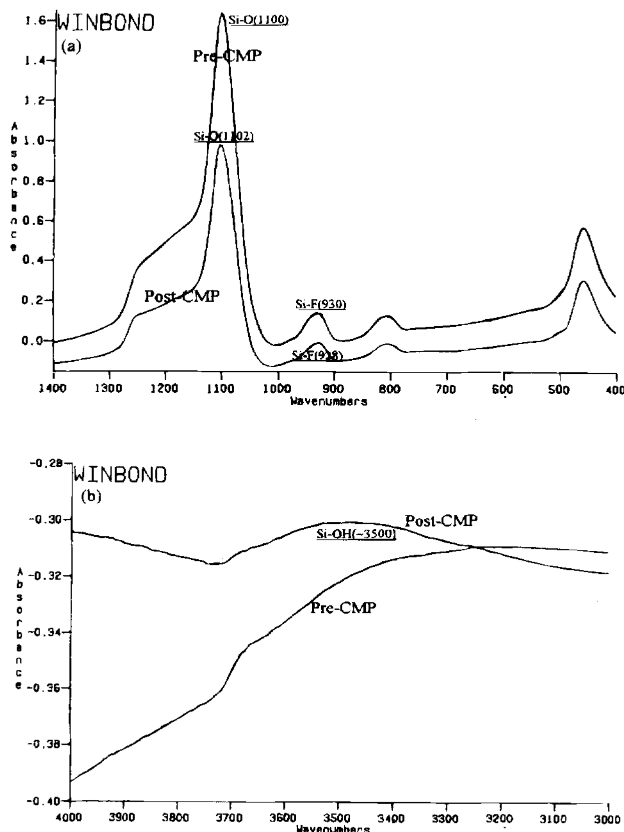

Fig. 6. Pre- and post-CMP FTIR spectra of SiOF with 8.9 a/o Si–F. (a) Wave number between 400 and 1400 cm^{-1}. (b) wave number between 3000 and 4000 cm^{-1}.

Also shown in Fig. 6b are the FTIR spectra over the wave number range between 3000 and 4000 cm^{-1}. It suggests that the OH– bonds have been formed on the SiOF film surface after CMP. These post-CMP R.I. increase and chemical bonding modifications due to moisture permeation may also correspond to an increase in dielectric constant,[17] manifesting the deterioration of low-K characteristics.

The mechanisms associated with the formation of OH– bonds and the deterioration of SiOF upon moisture absorption are not clear yet. Figure 7 is the scheme of our proposed bond reconstruction mechanism for the hydration of SiOF in an aqueous medium. As discussed previously, the incorporation of fluorine atoms results in the weakening of neighboring Si–O bonds. These weakened Si–O bonds would be vulnerable to the attack by OH– or H_2O. After the attack, the resulting silanol SiO_3–OH (left side of Fig. 7) groups would experience the reactions similar to the ones described in the model by Pietsch *et al.*[19] while the SiO_3–F (right side of Fig. 7) may undergo a series of hydration reactions as follows

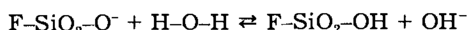

$$F\text{–}SiO_2\text{–}O^- + H\text{–}O\text{–}H \rightleftarrows F\text{–}SiO_2\text{–}OH + OH^-$$

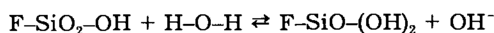

$$F\text{–}SiO_2\text{–}OH + H\text{–}O\text{–}H \rightleftarrows F\text{–}SiO\text{–}(OH)_2 + OH^-$$

$$F\text{–}SiO\text{–}(OH)_2 + H\text{–}O\text{–}H \rightleftarrows F\text{–}Si\text{–}(OH)_3 + OH^-$$

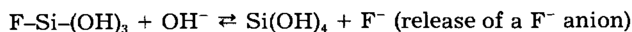

$$F\text{–}Si\text{–}(OH)_3 + OH^- \rightleftarrows Si(OH)_4 + F^- \text{ (release of a } F^- \text{ anion)}$$

As a result of these hydration reactions, Si–OH bonds are formed from the film surface while $Si(OH)_4$ radicals and F^- anions are released from it. The released fluorine anions would react with H_2O to form HF which etches the oxides again. Therefore, this phenomenon is termed a "self-assisted etching" mechanism as described previously. In addi-

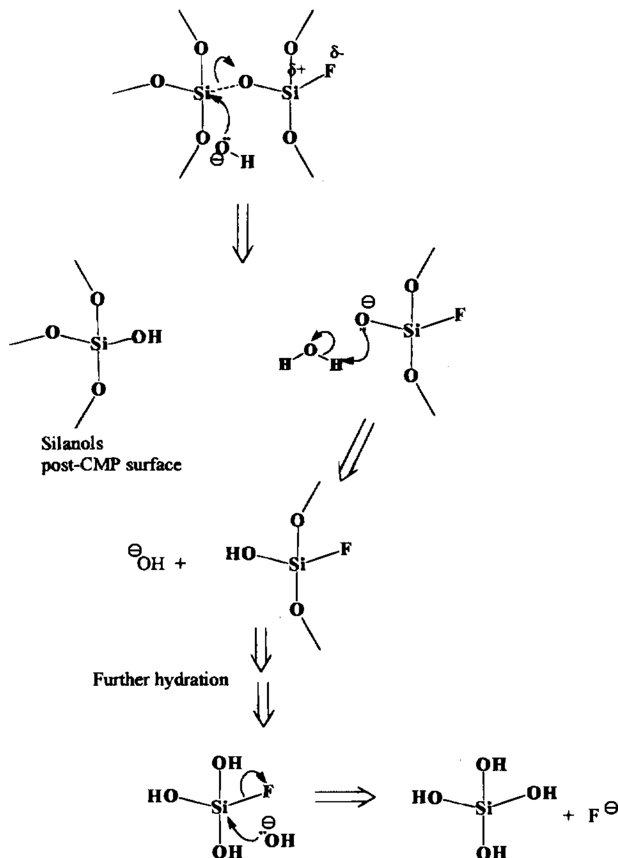

Fig. 7. The proposed bond reconstruction mechanism showing the hydration of SiOF.

Downloaded on 2014-04-28 to IP 140.113.38.11 address. Redistribution subject to ECS terms of use (see ecsdl.org/site/terms_use) unless CC License in place (see abstract).

tion, the release of fluorine may account for the increase in refractive index after CMP, as discussed earlier.

With regard to the mechanical part of CMP, hardness and elastic modulus of the thin films to be polished provide a quick and easy access to monitor the removal rate. The correlations between these two mechanical characteristics and the CMP removal rates of the undoped and fluorine-doped TEOS oxides are shown in Fig. 8. All quantities are normalized with respect to those of undoped TEOS so that their ratios are used to index the axes. A linear relationship exists between the hardness of these oxides and their CMP removal rate. In addition, the CMP removal rate is found to be inversely proportional to the elastic modulus, consistent with the prediction using the wear model by Liu and co-workers,[20] which can be simplified as

$$\text{Removal rate} = C \times \left(\frac{1}{E_a} + \frac{1}{E_f}\right) \times PV$$

where E_a and E_f are the moduli for the abrasives and the films to be polished, respectively; P is the down pressure, V is the rotation speed, and C is a coefficient related to slurry chemistry and other material characteristics. The results in Fig. 8 also indicate that under fixed chemistry and mechanical parameters, the CMP removal rate increases significantly with increasing fluorine content in the TEOS oxides due to the lower hardness and modulus in the SiOF films.

To successfully implement SiOF into the multilevel interconnect scheme, one has to engineer a process that is capable of achieving global planarization while maintaining the reliability and low-K characteristics of the SiOF. Based upon the results presented herein, the selection of a SiOF dielectric for IMD applications translates into trade-offs between CMP compatibility and low-K characteristics. A fluorinated oxide with 5.8 a/o Si-F and a dielectric constant of ~3.5 exhibits low compressive stress, reasonable mechanical strength, moderate CMP removal rate, and stable post-CMP characteristics, as evidenced from the data in Table I and Fig 5a. The combination of modern deposition techniques such as electron-cyclotron resonance (ECR)[21] and HDP-CVD,[22] and SiF_4 precursor has been demonstrated to produce highly stable fluorinated oxides which may be suitable for direct CMP operations. Another approach is to deposit a thin cap layer to protect the SiOF from moisture attack. Subsequently, another thicker IMD layer, such as TEOS oxide, is deposited on top of this cap layer and the normal CMP process can be practiced following the deposition to planarize the overall topography. Yet, this approach suffers from partial loss of low-K characteristics and increased process complexity. Further information on process integration issues of SiOF-CMP can be found elsewhere. Interested readers are directed to Ref. 17 for details.

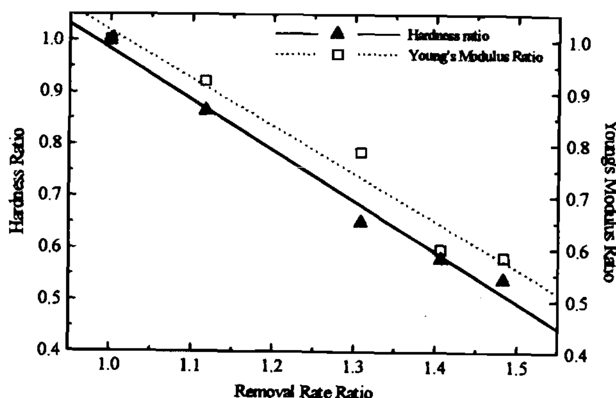

Fig. 8. The correlation between hardness and elastic modulus and CMP removal rate of SiOF. All quantities are normalized with respect to those of undoped TEOS oxides.

In summary, both the mechanical abrasion and chemical erosion are intensified during CMP of SiOF relative to undoped TEOS oxides because of the reduced hardness and enhanced chemical reactivity in the presence of fluorine in oxides. Likewise, the susceptibility of oxides to moisture and chemical attack is exacerbated as reflected on the post-CMP R.I. increase.

Conclusion

This work has demonstrated the sensitivity of the CMP removal rate to mechanical and chemical characteristics of fluorinated oxides. Fluorine doping into the PE-TEOS oxides reduces the hardness and elastic modulus while enhancing their chemical reactivity with acids and alkaline-based slurries compared with undoped TEOS oxides. Consequently, the CMP removal rate of these low-ϵ dielectrics is enhanced. Chemical bonding configurations may have been altered after CMP operations as evidenced from the changes in refractive index and shift in FTIR spectra. Similar to other dielectrics, the removal rate shows linear dependence on both hardness and modulus of the fluorinated oxides. A bond reconstruction mechanism is proposed to account for the hydration reactions occurring during moisture absorption of SiOF.

Acknowledgments

The authors would like to express their appreciation for insightful discussions with Dr. Chi-Wen Liu of the Taiwan Semiconductor Manufacturing Company (TSMC) Ltd. Gratitude is also given to Mr. Chuan-Ming Fang of the Chung-Cheng Institute of Technology for performing nanohardness measurements in the Precision Instrument Development Center in Hsinchu. This work is supported by National Science Council of Taiwan under Contract No. NSC 85-2622-E009-011.

Manuscript submitted June 19, 1996; revised manuscript received Dec. 5, 1996.

The National Chiao-Tung University assisted in meeting the publication costs of this article.

REFERENCES

1. B. Roberts, A. Harrus, and R. L. Jackson, *Solid State Technol.*, **38,** 69 (1995).
2. S. P. Murarka, *ibid.*, **39,** 83 (1996).
3. R. K. Laxman, *Semicond. Inter.*, **18,** 71 (1995).
4. P. Singer, *ibid.*, **19,** 88 (1996).
5. T. Usami, K. Shimokawa, and M. Yoshimaru, *Jpn. J. Appl. Phys.*, **33,** 408 (1994).
6. Y.-T. Hsieh, W.-T. Tseng, B.-T. Dai, T.-C. Chang, Y.-J. Mei, J.-D. Sheu, C.-F. Lin, M.-S. Feng, and H.-J. Yung, in *Proceedings of the Second International Dielectrics for VLSI/ULSI Multilevel Interconnection Conference (DUMIC)*, p. 287, Santa Clara, CA (1996).
7. T. Homma, T. Katoh, Y. Yamada, and Y. Murao, *This Journal*, **140,** 2410 (1993).
8. T. Homma, M. Suzuki, and Y. Murao, *ibid.*, **140,** 3591 (1993).
9. T. Homma, R. Yamaguchi, and Y. Murao, *ibid.*, **140,** 687 (1993).
10. T. Homma, *ibid.*, **143,** 707 (1996).
11. T. Homma, *ibid.*, **143,** 1084 (1996).
12. C.-P. Chen, C.-T. Lee, C.-F. Lin, H.-C. Yung, and L. Fang, in *Proceedings of the 1st International Chemical-Mechanical Polishing for VLSI/ULSI Multilevel Interconnection Conference (CMP-MIC)*, p. 82, Santa Clara, CA (1996).
13. W.-T. Tseng, C.-F. Lin, Y.-T. Hsieh, and M.-S. Feng, Paper presented in *1996 Materials Research Society Spring Meeting, Symposium*, K8.9, San Francisco, CA (1996).
14. I. Ali, S. Raghavan, and H. Risbud, *Semicond. Int.*, **13,** 92 (1990).
15. I. Ali, S. R. Roy, and G. Shinn, *Solid State Technol.*, **37,** 63 (1994).
16. C. S. Pai, J. A. Mucha, M. R. Baker, F. A. Baiocchi, and R. Liu, in *Proceedings of the Twelfth International VLSI Multilevel Interconnection Conference (VMIC)*, p. 406, Santa Clara, CA (1995).

Downloaded on 2014-04-28 to IP 140.113.38.11 address. Redistribution subject to ECS terms of use (see ecsdl.org/site/terms_use) unless CC License in place (see abstract).

17. W.-T. Tseng, Y.-T. Hsieh and C.-F. Lin, *Solid State Technol.*, **61**, (Feb. 1997).
18. F. Preston, *J. Soc. Glass Tech.*, **11**, 214 (1927).
19. G. J. Pietsch, Y. J. Chabal, and G. S. Higashi, *J. Appl. Phys.*, 78, 1650 (1995).
20. C.-W. Liu, B.-T. Dai, W.-T. Tseng, and C.-F. Yeh, *This Journal*, **143**, 716 (1996).
21. S. Lee and J.-W. Park, *J. Appl. Phys.*, **80**, 5260 (1996).
22. J.-H. Kim, S.-H. Seo, S.-M. Yun, H.-Y. Chang, K.-M. Lee, and C.-K. Choi, *This Journal*, **143**, 2990 (1996).

Analysis of Bonding-Related Gas Enclosure in Micromachined Cavities Sealed by Silicon Wafer Bonding

S. Mack,[a] H. Baumann,[b] U. Gösele,[a] H. Werner,[c] and R. Schlögl[c]

[a]*Max-Planck-Institute of Microstructure Physics, D-06120 Halle (Saale), Germany*
[b]*Robert Bosch GmbH, D-72703 Reutlingen, Germany*
[c]*Fritz-Haber-Institute, D-14195 Berlin-Dahlem, Germany*

ABSTRACT

We investigated the bonding-related gases trapped inside the cavities of micromachined silicon test structures that had been sealed by silicon direct bonding or anodic bonding under vacuum conditions. The gas content inside the cavities was analyzed by quadruple mass spectroscopy. The magnitude of the residual gas pressure inside the cavities for different cavity layouts and for various bonding processes was monitored. In cavities bonded by low-temperature silicon direct bonding the residual gases are reaction products originating from the mating silicon surfaces during annealing. Inside the cavities mainly H_2, H_2O, and N_2 are found. The total gas pressure is primarily determined by the H_2 component. Cavities sealed by anodic bonding mainly contain O_2, which originates from mobile oxygen ions inside the bonding glass. The residual gas pressure inside anodically bonded cavities depends neither on the applied bonding voltage nor on the bonding area surrounding each cavity.

Introduction

Silicon micromachining has gained importance lately as a manufacturing process for mechanical components that are inexpensive and can be batch-processed in large quantities. Many micromechanical applications need the hermetical vacuum sealing of cavity structures. This can be accomplished on a wafer basis by silicon wafer bonding under vacuum conditions. The two dominant bonding technologies are silicon direct bonding (SDB) and anodic bonding (AB).[1] SDB is a process whereby two silicon wafers are mated together at room temperature and then annealed to achieve a higher bond strength.[2] AB is mainly employed in joining a silicon and a glass wafer by applying a dc voltage across the silicon/glass sandwich.[3]

For vacuum enclosure, wafer bonding is performed under reduced pressure in a vacuum chamber. It is known that the residual gas pressure inside the cavity after bonding is considerably higher than the original chamber pressure.[1] Two gas sources may be responsible for this effect. Reactions occurring during the bonding process can lead to the generation of gaseous reaction products. Another source could be the desorption of gases from the bond interface and from the inner surfaces of the cavity.

The released gases are trapped inside the cavities and critically influence the device performance of micromechanical applications. For example, the frequency response of mechanical oscillating parts inside the cavity is strongly dependent on the residual gas pressure.[4] Additionally, the gas content is of interest, since the enclosed gases may cause corrosion inside the cavities.[5]

Only a few process ideas to minimize the gas pressure enclosed inside the cavities have been reported in the literature.[1] All of them concentrate on the removal of the generated gases after the bonding process and do not focus on the prevention of the gas evolution process itself. Yoshimi *et al.*[6] realized very small residual gas pressures by placing a getter material inside the cavities.

Gas generation at the interface of directly bonded silicon wafers takes place during annealing and is strongly temperature dependent.[7] Gases trapped at the bonding interface are assumed to be the cause of poor low-temperature bonding strength.[8] For unstructured silicon wafers the gas generation manifests itself in the formation of bonding defects, the so-called interface bubbles.[9] It is presumed that interface bubbles are filled with H_2, H_2O, and gaseous hydrocarbons. Anodic bonding of thin glass wafers to a silicon substrate also results in the formation of bubble-like voids speculated to be due to gases evolved from the glass.[10] Alkali oxide-containing glasses as employed for anodic bonding are known for oxygen evolution during application of a dc potential to the glass.[11] Based on this observation a high oxygen content inside anodically bonded cavities is expected.

To our knowledge the present report is the first one on the nature of the gases enclosed inside the cavities after bonding in vacuum. There is one report[12] in the literature that deals with the analysis of the gas content of cavities directly bonded under normal atmospheric conditions. However, in this case it was not possible to identify clearly whether the observed gases resulted from the enclosed atmosphere or from interfacial reactions.

We investigated the bonding-related gas generation and its dependence on various bonding parameters. The gas content inside the cavities of pressure sensor test structures was analyzed by quadruple mass spectroscopy (QMS). For this purpose bonded cavities were opened in ultrahigh vacuum (UHV) by breaking the silicon mem-

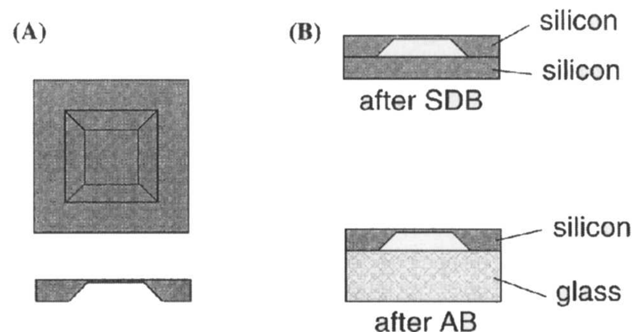

Fig. 1. (A) Test structure cavity that was used in the low-temperature SDB and in the AB experiments (schematic top view and cross section). (B) Sealed cavity after bonding (cross section).

Downloaded on 2014-04-28 to IP 140.113.38.11 address. Redistribution subject to ECS terms of use (see ecsdl.org/site/terms_use) unless CC License in place (see abstract).